Mathematical Biology and Bioinformatics
2024. V. 19. № 2. P. 261–275. doi: 10.17537/2024.19.261

========== **MATHEMATICAL MODELING** ==========

Cationic Biocides Tend to Embed into the Inner Layer of the Model Outer Membrane Vesicles of Gram-negative Bacteria: Computational Insights

Kholina E.G., Kovalenko I.B., Strakhovskaya M.G.

Lomonosov Moscow State University, Moscow, Russia

Abstract. The outer membrane vesicles (OMVs), produced by many pathogenic bacteria, play a significant role in bacterial pathogenesis. They promote bacterial resistance to antibiotics and act as natural protective barriers. The study of OMVs is essential both for understanding the general mechanisms of bacterial pathogenicity and for the development of the antibacterial drugs. In this paper, we created model vesicle that imitate the OMVs of Gram-negative bacteria using molecular modeling techniques. To investigate the interaction of the cationic antimicrobial compounds with the outer lipopolysaccharide (LPS) monolayer and the inner phospholipid monolayer of the OMV membrane, we performed molecular dynamics simulations by placing molecules of the cationic antiseptic octenidine on the outside or inside of model vesicles. The interaction of octenidine with the outer and inner monolayer was significantly different: octenidine interacted weakly with the outer LPS surface of the model OMV, but exhibited high affinity for the phospholipids of the inner monolayer. To study the translocation of cationic antimicrobial molecules within model OMV, we performed steered molecular dynamics simulations. For all three cationic biocide molecules, antiseptic octenidine, photosensitizer octakis(cholinyl)zinc phthalocyanine, and dye methylene blue, it turned out that, along with the LPS of the outer membrane of the OMV, the phosphates of lipid A molecules represent the final barrier to their penetration into the model OMV.

Key words: *octenidine, octakis(cholinyl)zinc phthalocyanine, methylene blue, Gram-negative bacteria, outer membrane vesicles, lipopolysaccharides, coarse grain modeling, MARTINI.*

INTRODUCTION

Antimicrobial resistance is one of the largest public health threats worldwide. Infections associated with resistant pathogens are projected to cause 10 million deaths annually by 2050 [1]. The vast majority of dangerous infectious pathogens are Gram-negative bacteria (GNB), including *Acinetobacter baumannii*, *Escherichia coli*, *Pseudomonas aeruginosa*, *Klebsiella pneumoniae*, and other species. These bacteria have a wide range of intrinsic and acquired resistance mechanisms [2–5], making them resistant to many biocides, antibiotics, antiseptics, disinfectants, and antimicrobial peptides. Strategies for bacterial resistance include preventing biocides from accessing cells and from penetrating the cell wall, pumping from the cell, as well as neutralizing and chemically inactivating biocide molecules and modifying their cellular targets.

GNB have several important intrinsic and acquired resistance mechanisms related to the cell wall and its derivatives. GNB have a unique structure – a complex cell wall, consisting of two membranes – outer and cytoplasmic, between which there is a layer of peptidoglycan in the periplasmic space. The lipid composition of the outer membrane differs from the cytoplasmic membrane. It is asymmetrical: the outer monolayer consists of lipopolysaccharides (LPSs) and the inner monolayer consists of phospholipids. LPSs provide

protection to GNB cells both at the level of the O-antigen, long polysaccharide chains that protrude into the external environment and are capable of trapping harmful molecules, preventing them from entering the cell, and at the level of the core region and polar heads of lipid A molecules, which create an energy barrier to the translocation of unwanted molecules through the cell wall [6, 7].

Outer membrane vesicles (OMVs), which are cell wall derivatives, play an important protective role in addition to other extracellular structures such as capsules, exopolysaccharides, and biofilm matrix components. OMVs formation is common and characteristic of GNB [8]. Almost all GNB species, including representatives of the ESKAPE group of pathogens, produce OMVs [9]. OMVs have a diameter of 20–250 nm [10–12]. These vesicles form as protrusions of the outer membrane and bud from the bacterial cell. Their outer monolayer consists mainly of LPSs, and the inner monolayer consists of phospholipids. Proteins of the outer cell membrane are also embedded in the OMVs [10]. These vesicles also contain components of the periplasmic space, in particular, proteases, detoxification enzymes, and nucleases [13]. OMVs perform various functions important for bacterial cells [14–17], including transferring toxins [18–20], surface adhesins [21, 22], and virulence factors [15, 23]; cleaving extracellular material into simple molecules utilized for bacterial metabolism [24]; capturing metals, such as iron [25]; and removing protein aggregates and toxicants from the cell [15, 26]. OMVs can also serve as a biofilm nucleation factor, they maintain cohesion inside biofilms [8, 27] and provide communication between bacterial cells [28]. In addition to these functions, it is worth noting that OMVs can protect bacteria against antimicrobial substances through three main mechanisms: 1) encapsulation of antibiotics and their removal from the cell; 2) direct binding of antibiotics to the surface of OMVs; and 3) destruction of antibiotic molecules entering the OMV due to the action of periplasmic enzymes [29]. In particular, OMVs produced by *Acholeplasma laidlawii* have been shown to contain fluoroquinolone antibiotics such as ciprofloxacin [30], and OMVs produced by *Pseudomonas aeruginosa* contain aminoglycosides such as gentamicin [31], indicating that OMVs can remove antibiotics from the cell. OMV components can also directly bind antibacterial compounds. For example, compared with the wild type, the isogenic hyper-vesiculating *yieM* mutant of *Escherichia coli* demonstrated better survival after exposure to the cyclic cationic antimicrobial peptides polymyxin B and colistin [32], chicken cathelicidin CATH-2, human cathelicidin LL-37, and cathelicidin porcine PMAP-36 [33]. Moreover, addition of purified OMVs to bacterial culture reduced the sensitivity of wild-type *E. coli* to cationic antimicrobial peptides.

In A. baumannii, OMVs derived from polymyxin B-resistant strains provided protection to polymyxin B-sensitive strains [34]. In addition to resistance to antimicrobial peptides, OMVs can also confer resistance to other biocides. For example, OMVs from *Porphyromonas gingivalis* can capture the cationic antiseptic chlorhexidine [35]. The degradation of antimicrobial molecules within OMVs is supported by evidence that these vesicles may contain enzymes capable of degrading β-lactam antibiotics [13, 36, 37].

Studying the interactions of various biocides with OMVs is critical to understanding how this GNB pathogenicity factor functions. This, in turn, will help improve efficiency and develop new effective antibacterial drugs. Furthermore, OMVs can be used as containers for drug delivery [28]. This requires a detailed study of the interactions of compounds with different physicochemical properties with the LPS surface of OMVs, the translocation of antimicrobial agents into vesicles, their distribution within the internal vesicular space, and interactions with the inner phospholipid leaflet of OMV.

In silico molecular model systems have made significant contributions to the development of antimicrobial agents. The MARTINI coarse-grained force field [38] is a powerful tool for studying the structure and dynamics of bacterial membranes [7, 39–41], as well as for studying intermolecular interactions and the underlying mechanisms of action of antimicrobials [42–49]. Because this force field uses particles composed of 3–4 heavy atoms

instead of individual atoms, it allows the study of large molecular dynamics systems, such as model liposomes, on time scales on the order of microseconds.

In this study, within the MARTINI force field, we created a liposome model mimicking OMVs of GNBs. We compared the interactions of three different antimicrobials (the antiseptic octenidine, the photosensitizer octakis(cholinyl)zinc phthalocyanine, and the dye methylene blue) with model OMVs. Of particular interest was the study of the interactions of the cationic antiseptic octenidine in realistic concentrations, used in medical solutions, with both the external and internal surfaces of the OMV model.

MATERIALS AND METHODS

A coarse-grained molecular dynamics model of OMV with asymmetric lipid composition was created using CHARMM-GUI Martini Maker [39] in MARTINI force field [38] and had an internal radius of 12 nm. The outer monolayer of the model vesicle consisted of 919 rough (Ra) LPS (RAMP) [50] molecules, while the inner monolayer consisted of 1,273 neutral palmitoyl oleoyl phosphatidylethanolamine (POPE), 70 negative cardiolipin (CDL2), and 70 negative palmitoyl oleoyl phosphatidylglycerol (POPG) lipids. The composition of the model OMV was chosen based on [39]. The model OMV placed in the simulation box is shown in Figure 1.

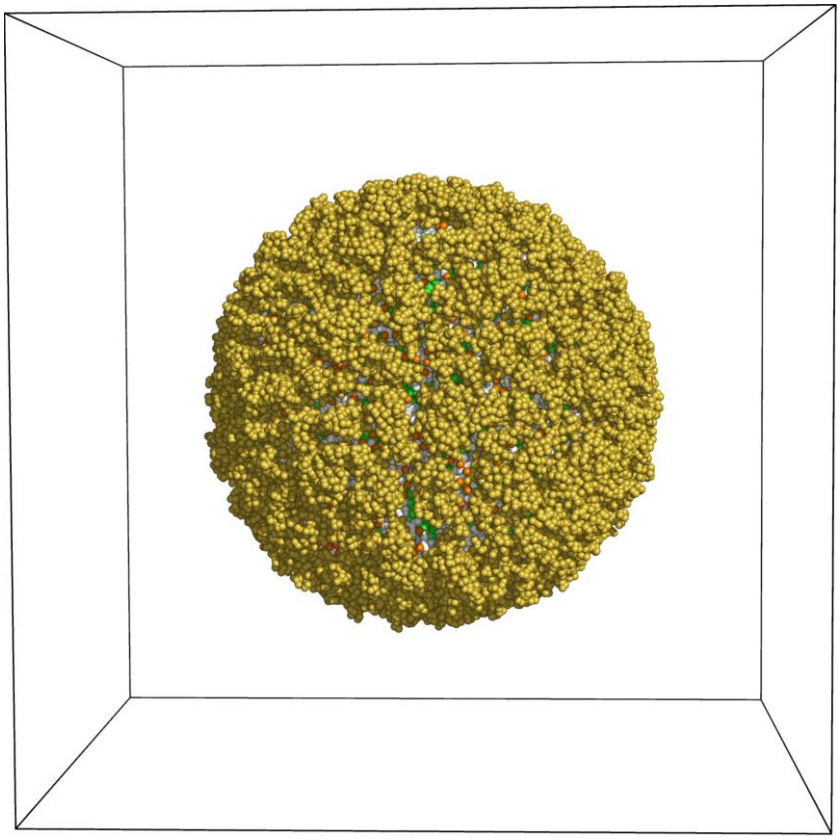

Fig. 1. The model OMV placed in the simulation box (molecules of water and ions are not shown).

In equilibrium molecular dynamics simulations, octenidine molecules were added to the simulation box either outside the OMV or inside its interior volume at an antiseptic:lipid ratio of 1:4 or 1:8, respectively, given that there are approximately three lipid molecules per LPS molecule in the bacterial outer membrane [51, 52]. Because octenidine molecules rapidly aggregated, to reduce the box size, aggregates of octenidine obtained during auxiliary molecular dynamics simulations were randomly placed into the model vesicle as described above.

The model OMV with six pores was created following the conventional approach for building a vesicle using CHARMM-GUI Martini Maker. After energy minimization, molecular dynamics simulations of the OMV with open pores were performed for 1 μs. Position restrictions were applied to the OMV molecules to ensure uniform distribution of ions inside and outside the OMV. Molecular dynamics simulations were performed in the NPT ensemble with an integration step of 20 fs using a V-rescale thermostat (T = 320 K, τ_t = 1.0 ps) and a Parrinello-Rahman barostat (time constant = 12.0 ps, compressibility = 3×10^{-4} bar $^{-1}$) with a polarizable water model (ε_r = 2.5) [53] and with the addition of Na^+/Cl^- ions at a concentration of 150 mM. Molecular dynamics calculations were performed using the Gromacs 2022.4 software [54]. To estimate the internal volume of the model vesicle, ProKSim (Protein Kinetics Simulator [55, 56] software was used. We used PyMOL [57] to visualize the molecular structures.

To elucidate the translocation pathways of three different antibacterial compounds (the antiseptic octenidine, the photosensitizer octakis(cholinyl)zinc phthalocyanine, and the dye methylene blue) into the model OMV, we used steered molecular dynamics. To obtain force profiles during the translocation of biocides inside the model OMV, the center of mass of each biocide was pulled along the radius of the model OMV at a constant velocity of 1 nm/ns. The value of the harmonic spring of the force constant was 10.000 kJ mol^{-1} nm^{-2}. Coarse-grained molecular dynamics models of octakis(cholinyl)zinc phthalocyanine, octenidine, and methylene blue have been created earlier [58–60]. Details of the molecular dynamics systems are presented in Table 1.

Table 1. Details of the molecular dynamics (MD) systems

MD system number	Type of MD simulations	Biocide	Number of biocide molecules	Number of water molecules	Box size, nm
1	Equilibrium MD	Octenidine (outside the OMV)	675	771.062	46.2 × 46.2 × 46.2
2	Equilibrium MD	Octenidine (inside the OMV)	175	675.379	44.3 × 44.3 × 44.3
3	Steered MD	Octenidine	1	680.081	45.7 × 45.7 × 45.7
4	Steered MD	Octakis(cholinyl)zinc Phthalocyanine	1	679.937	45.7 × 45.7 × 45.7
5	Steered MD	Methylene blue	1	680.103	45.7 × 45.7 × 45.7

RESULTS

Interaction of the cationic antiseptic octenidine with the outer LPS monolayer of the model OMV

Using the molecular dynamics model (1) (Table 1), we studied the interaction of the antiseptic octenidine and the outer LPS monolayer of the model OMV for 2.3 μs. During the simulation, antiseptic aggregates that were initially randomly placed outside the OMV collided with each other, aggregating and forming clusters of more molecules. At the beginning of the simulation, clusters of only 25 molecules were present (Figs. 2,a and Fig. 3). After about 20 ns, the clusters began to merge in pairs, then in groups of three at 50 ns, and by 100 ns, four clusters had merged into a larger cluster (Fig. 3). After 2 μs of simulation, the initial clusters had almost disappeared, with the largest clusters consisting of more than 100 octenidine molecules (Figs. 2,b and Fig. 3). The aggregates were not stable and, during molecular dynamics, were sometimes adsorbed onto OMV, dissociated from the vesicle surface, and merged with other aggregates. However, the key point was that they not only did

not penetrate the model vesicle but also did not reach the core region of the LPS molecules in the outer monolayer of OMV. As a result, we can conclude that even the outer bacterial membrane, consisting of rough LPS molecules without O-antigens, acts as a reliable barrier to the penetration of biocide into OMVs and bacterial cells.

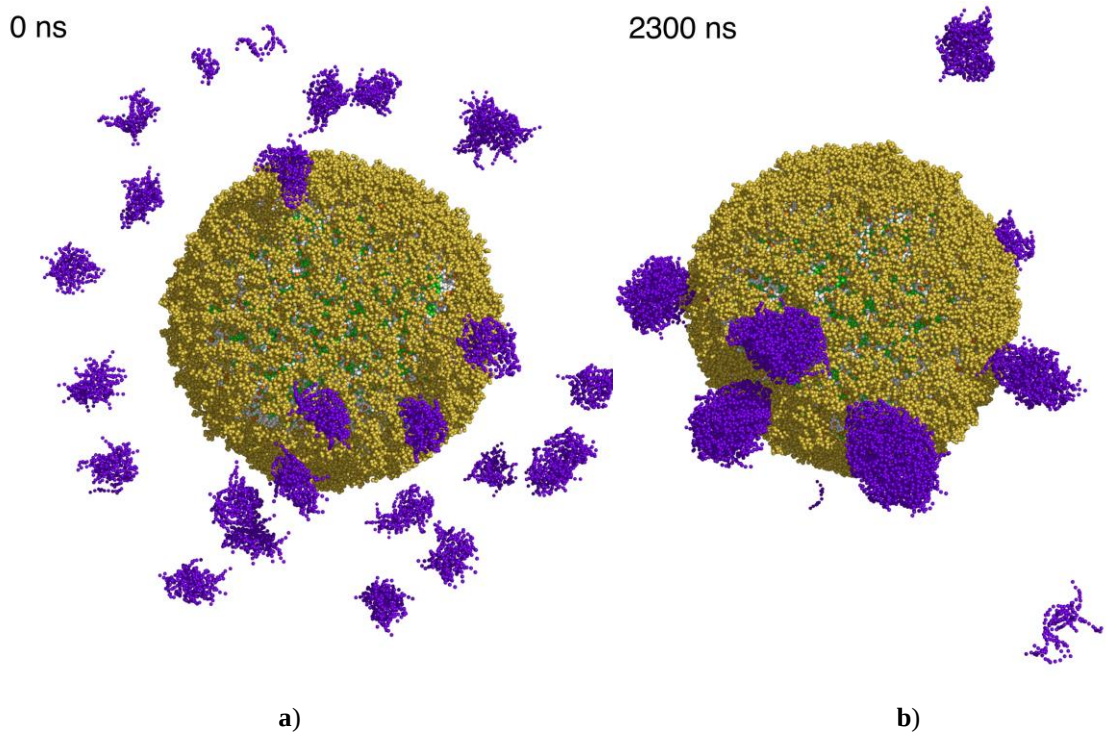

a) **b**)

Fig. 2. Interaction of octenidine (shown in purple) with the outer surface of the model OMV: snapshots of molecular dynamics simulation at initial time (**a**) and 2300 ns (**b**).

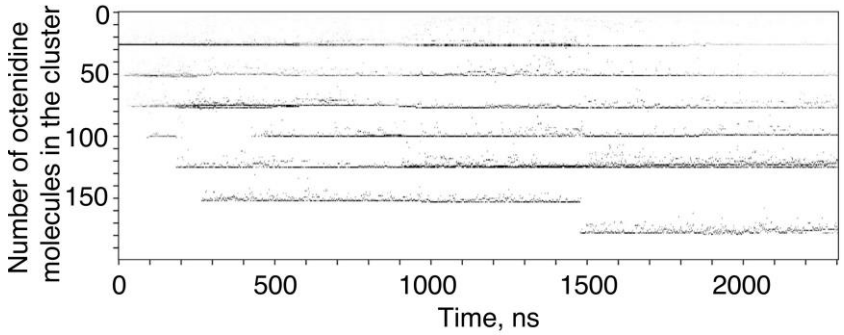

Fig. 3. Aggregation of octenidine molecules during interaction with the outer surface of the model OMV.

Outer LPS monolayer as a barrier to the translocation of several types of cationic biocides into the model OMV

The translocation of the three biocides into the model OMV was studied using molecular models (3)–(5) (Table 1) via steered molecular dynamics. To simulate this process, molecules of various chemical groups were selected, including the cationic antiseptic octenidine, the photosensitizers octakis(cholinyl)zinc phthalocyanine, and the dye methylene blue (Fig. 4). Octakis(cholinyl)zinc phthalocyanine is a macrocyclic compound derived from zinc phthalocyanine with eight peripheral choline substituents, whereas octenidine is a dipyridine derivative, a linear molecule with a flexible linker between two pyridine groups; methylene blue is a heterocyclic phenothiazine dye. The molecules studied differed in charge, shape, and

size. In particular, octakis(cholinyl)zinc phthalocyanine has a charge of +8, octenidine +2, and methylene blue +1.

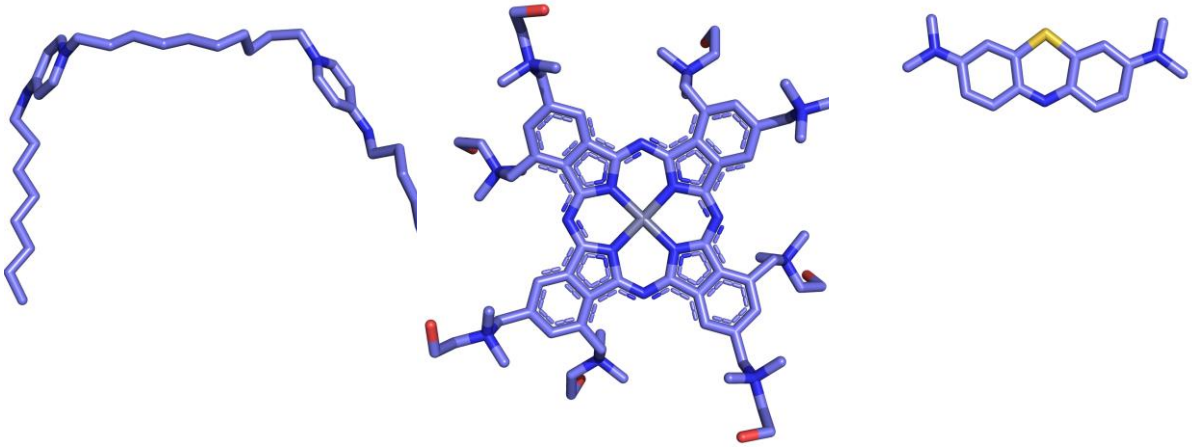

a) **b**) **c**)

Fig. 4. Spatial structures of the studied biocides: the antiseptic octenidine (**a**), the photosensitizer octakis(cholinyl) zinc phthalocyanine (**b**), the dye methylene blue (**c**).

When the octenidine molecule entered the outer core region of the LPS molecules of the OMV outer monolayer at 5 ns, the maximum force was approximately 600 pN (Fig. 5,a). The high force is due to electrostatic contact between the positively charged octenidine molecule and the negatively charged groups of the core region and the lipid A phosphates of the LPS molecules. Further, after passing through the outer monolayer of the vesicle, the force rapidly decreased due to the weakening of electrostatic interactions with the outer LPS monolayer of the OMV and reached approximately 200 pN within approximately 9 ns, which corresponds to the release of the octenidine molecule into the vesicle.

When a octakis(cholinyl) zinc phthalocyanine molecule was pulled through a model vesicle (Fig. 5,b), the force increased to approximately 1500 pN. This value is 2.5 times greater than that of octenidine since the octakis(cholinyl) zinc phthalocyanine molecule is larger in size and mass (1395 Da versus 553 Da for octenidine), and has a stronger positive charge (+8 versus +2 for octenidine). Furthermore, these compounds have fundamentally different chemical structures and geometries: the phthalocyanine molecule contains a rigid macrocyclic ring with peripheral substituents, whereas the octenidine molecule is linear and flexible.

The highest force for methylene blue when pulled into the model OMV was approximately 300 pN (Fig. 5,c), which is 5 times less than that of octakis(cholinyl) zinc phthalocyanine and 2 times less than that of octenidine. This corresponds to the smaller size, mass (284 Da), and electrical charge (+1) of the methylene blue molecules.

Thus, the LPSs of the outer monolayer of the model vesicle, containing a significant amount of negatively charged groups, act as a barrier to the translocation of all studied biocide molecules into the OMV.

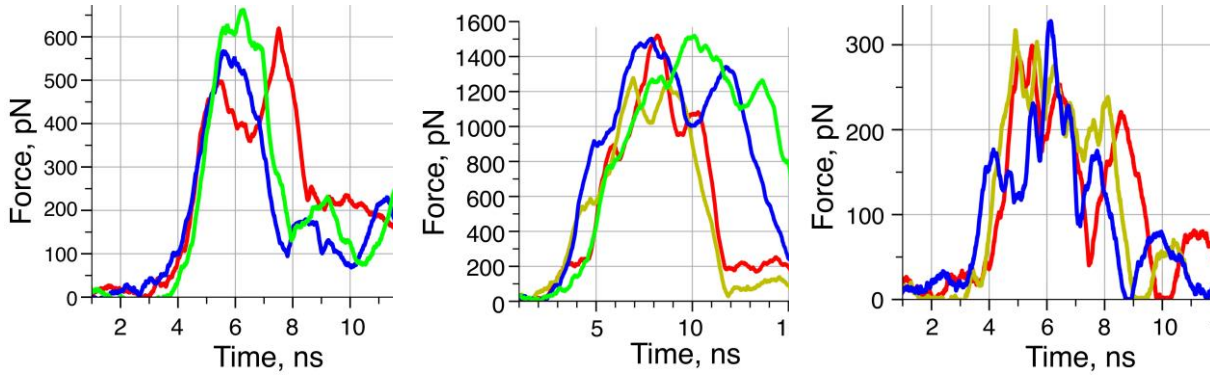

a) **b**) **c**)

Fig. 5. Force profiles for the translocation of octenidine (**a**), octakis(cholinyl) zinc phthalocyanine (**b**), and methylene blue (**c**) into the model OMV. Force profiles for independent runs of steered molecular dynamics are shown in different colors.

Interaction of the cationic antiseptic octenidine with the phospholipid monolayer of the model OMV

Since the translocation of the antiseptic octenidine into the model vesicle did not occur for approximately 2 μs, a molecular dynamics system (2) was studied in which, at the initial time, octenidine molecules were placed directly into the internal volume of the model vesicle (Fig. 6,a). The interaction of octenidine with the inner phospholipid leaflet was radically different from its interaction with the outer LPS monolayer (Fig. 6). Thus, the process of octenidine molecules embedding into the inner monolayer of OMV with the simultaneous disintegration of the aggregates began almost immediately. After approximately 500 ns, most of the octenidine molecules detached from the aggregates and embedded into the lipid monolayer (Fig. 6,b). At this time, one large aggregate containing more than 50 molecules still existed, but it completely disappeared after 2 μs, since its molecules were also embedded in the phospholipid monolayer (Fig. 6,c). After 4 μs, octenidine molecules were evenly distributed throughout the lipid monolayer (Fig. 6d). This is also illustrated by the average distance between the centers of mass of individual octenidine molecules and the center of mass of the model vesicle (Fig. 7,a). The plot shows that the number of octenidine molecules incorporated into the inner monolayer increases significantly shortly after the start of the simulation. By 500 ns, more than half of the octenidine molecules had already embedded into the monolayer, and by 2 μs, almost all the molecules had embedded, as evidenced by the average distance between the centers of mass of individual antiseptic molecules and the center of the model vesicle slightly exceeding 80 Å, which approximately corresponds to the internal radius of the OMV.

To assess the effect of the antiseptic on the structural characteristics of the OMV during its interaction, the internal volume of the model vesicle was measured. To do this, the entire internal volume was divided into cubic cells 1 Å in size, and the number of cells containing the solvent was counted. The internal volume of the model vesicle changed slightly during the molecular dynamics simulation. Initially, the internal volume of the vesicle was 2.045 nm^3, which decreased to a value of 1.980 nm^3 in 4 μs. A visualization of the internal volume of the OMV in several molecular dynamics frames is shown in Figure 7,b.

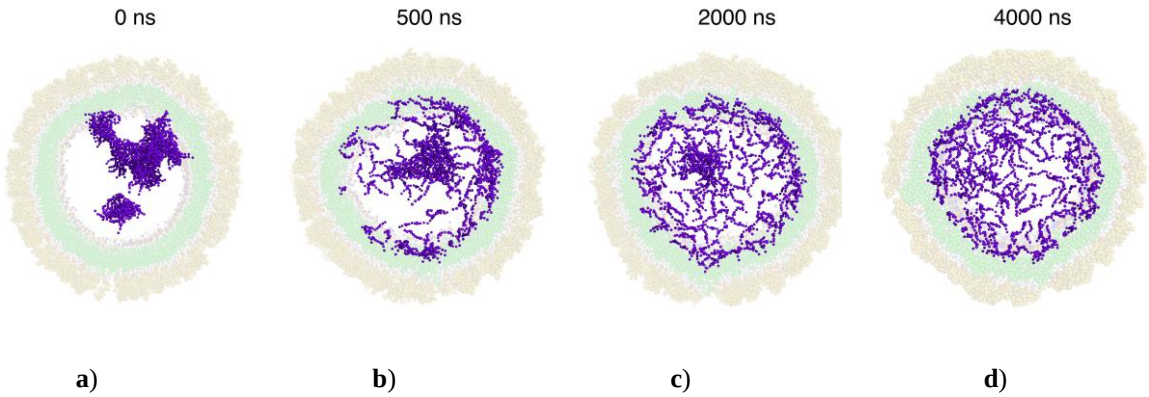

Fig. 6. Interaction of octenidine with the phospholipid monolayer of the model OMV: snapshots of molecular dynamics simulation at initial time (**a**), 500 ns (**b**), 2000 ns (**c**), and 4000 ns (**d**). The core region of LPS molecules is shown in beige, acyl chains of lipid A of the outer monolayer and lipids of the inner monolayer are shown in green, and octenidine molecules are shown in purple.

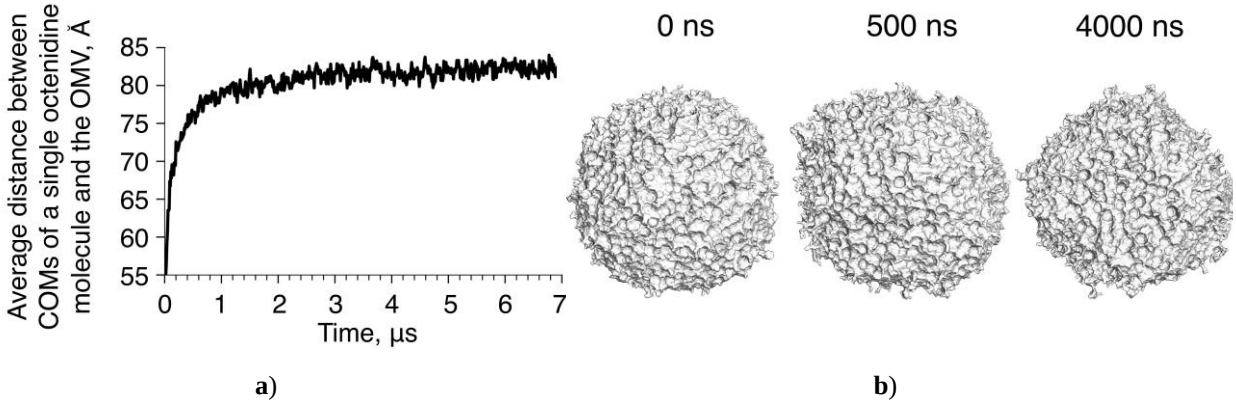

Fig. 7. Interaction parameters of octenidine with the phospholipid monolayer of the model OMV. Average distance between the center of mass (COM) of each single octenidine molecule and the COM of the model OMV during the molecular dynamics simulation (**a**). Visualization of the internal volume of the model vesicle during molecular dynamics.

DISCUSSION

In this work, we created a coarse-grained molecular dynamics model of a vesicle, the outer layer of which consists of LPSs and the inner monolayer of phospholipids. The model is similar in structure and lipid composition to OMVs of GNBs, which originate from the outer membrane of the bacterial cell wall. The permeability barriers of these bacteria are designed to reliably prevent biocides with different physicochemical characteristics from entering the cell [61, 62]. The outer layer of OMVs is built mainly of LPS molecules, which contain O-antigen chains that extend outward and can reach tens of nanometers in length. These O-antigens are composed of repeating units with varying net charge and hydrophobicity. O-antigen chains serve an important function in initial line of bacterial defense by acquiring antimicrobial chemicals away from the cell surface [63]. The core region of LPS molecules has negative charges, which are partially neutralized by inorganic calcium and magnesium ions, which bind and strengthen the LPS monolayer. The next barrier to antimicrobial compounds is lipid A. The polar heads of these glycolipids act as an energy barrier to hydrophobic molecules, making penetration more difficult than that of phospholipids [7, 41]. Lipid A molecules, in addition to glucosamine, contain saturated acyl chains. These chains have limited fluidity, which reduces the diffusion rate of lipophilic compounds by 50–100 times. OMVs are miniature copies of bacterial cell walls with characteristic physicochemical properties. These vesicles are capable of binding biocide molecules at a distance from the

parent cell, protecting them from damage. Previously, we created models of flat bilayer membranes containing LPSs of *P. aeruginosa* either with negatively charged O5 O-antigens or with neutral polyrhamnose antigens [60]. Using these models, we showed that the photosensitizer octakis(cholinyl)zinc phthalocyanine, when interacting with a membrane containing negatively charged antigens, electrostatically binds to antigenic chains and does not reach the core region of LPS molecules. In the case of LPS membranes with polyrhamnose charge-neutral antigenic chains, metallophthalocyanine molecules practically do not bind to antigens and also do not reach the core of the LPSs. For smaller and less charged methylene blue molecules, the antigens of both types do not constitute an absolute barrier to octacationic zinc phthalocyanine. Molecular dynamics simulations demonstrated that individual methylene blue molecules can penetrate to the outer saccharides of the LPS core region.

Thus, LPS antigens may create a primary barrier to the penetration of antimicrobial compounds. However, it was found that in chronic infections with *P. aeruginosa* [64] and when exposed to high temperatures [65], antigens are not produced and are not present in LPS membranes. Additionally, the distribution of LPS molecules in the outer membrane is irregular, which leads to the formation of areas with rough LPSs that lack antigens [66]. Therefore, it would be interesting to investigate whether rough LPSs itself could create a barrier to biocide permeation. In this work, we investigated the barrier properties of OMV containing rough LPS molecules in the outer monolayer, in the presence of the cationic antiseptic octenidine. Octenidine is an aminopyridine derivative and bears two positive charges connected by a flexible hydrophobic alkyl linker [67]. Octenidine has antibacterial activity against a wide range of bacteria [68]. During our molecular dynamics simulations, we observed that when octenidine interacts with the outer surface of OMVs, it forms large aggregates containing more than 100 molecules. These aggregates are sometimes adsorbed on the OMV surface. However, they do not penetrate inside the model vesicle, even into the core region of the LPS molecules (Fig. 2, 3).

Given that in our previous study [60], small molecules such as methylene blue reached the core region of LPSs, it was interesting to study the contribution of the core region and lipid A in forming a barrier to the penetration of cationic biocides. To this end, we compared the translocation of the photosensitizer octakis(cholinyl) zinc phthalocyanine, the antiseptic octenidine, and the dye methylene blue into the model OMV.

The equilibrium molecular dynamics results (Fig. 2) are consistent with the translocation profiles of octenidine inside the model OMV (Fig. 5,a), which show that a significant force of 600 pN must be applied to the center of mass of octenidine to ensure its transport across the LPS-containing membrane of the model vesicle. The greatest force required to pull methylene blue into the OMV was approximately 300 pN. This is compatible with the lower mass (284 Da vs. 553 Da for octenidine), and lower electric charge (+1 vs. +2) of the methylene blue molecule. It is noteworthy that when modeling flat LPS membranes, individual methylene blue molecules can reach the core region of LPSs and even be partially incorporated into them [60]. This corresponds to half the peak force observed in the translocation profiles of methylene blue (Fig. 5,c) compared to that of octenidine (Fig. 5,a). When octakis(cholinyl) zinc phthalocyanine was pulled into the model vesicle, the force increased to approximately 1500 pN (Fig. 5,b). This number is 2.5 times greater than that of octenidine, presumably because the zinc phthalocyanine molecule is larger in size and mass (1395 Da versus 553 Da for octenidine) and has a stronger positive charge (+8 vs. +2 for octenidine). Methylene blue has 4.5 times less mass and 8 times less charge than zinc phthalocyanine, and its peak forces were 5 times lower when translocated into the model OMV. In addition, the studied biocides have fundamental differences in chemical structure and geometry. The photosensitizer based on zinc phthalocyanine is a macrocyclic compound with a rigid structure and eight peripheral choline substituents. On the other hand, the antiseptic octenidine is a linear and flexible molecule due to the presence of an alkyl linker

connecting positive charged groups. The photosensitizer methylene blue is a aromatic thiazine heterocycle with a rigid structure that carries a delocalized positive charge. Similarly, for the three biocides studied, the maximum force corresponds to the moment when the positive charges of the biocides are released from the phosphates of the lipid A molecules, which represents the final barrier to their penetration into the OMV.

The discovery of considerable barriers of 300–600 pN for methylene blue and octenidine suggests that these biocides may enter the bacterial cells via an alternate pathway. It is believed that biocides with a molecular weight of up to 600 Da penetrate the outer membrane of GNB through porin channels and have an antibacterial effects on the bacterial plasma membrane and intracellular structures [6, 69]. However, the potential effects of biocides located in the periplasmic space on the phospholipid monolayer of the outer membrane are not fully understood. To simulate the situation where biocides reside in the periplasm or intravesicular space, 175 octenidine molecules were placed in a model OMV with an internal diameter of 24 nm. The interaction of octenidine molecules with the inner lipid monolayer was significantly different from the interaction with the outer LPS monolayer. The process of incorporation of octenidine molecules into the inner monolayer was rapid: more than half of all molecules were integrated in 500 ns and almost all in 2 μs (Figs. 6, 7). That is, octenidine practically does not interact with the outer LPS surface of the model vesicle, but has significant affinity for the lipids of its internal monolayer. Thus, the results of our modeling showed that OMVs, as a way to protect the bacterial cells from unwanted compounds, are able of capture and retain biocide molecules from the periplasmic space of the cell. The ability of OMVs to encapsulate cationic antiseptic molecules within the intravesicular space suggests that vesiculation may help reduce biocide concentrations in the periplasm. As a result, membranotropic biocides will become less effective and have less bactericidal effect.

Our molecular dynamics results showed that the incorporation of antiseptic into the inner monolayer resulted in a small change in the geometry of the model vesicle. This is clearly visible at a long simulation time of 4 μs when visualizing the internal volume of the model OMV (Fig. 7,b). However, despite minor changes in morphology, the integrity of the model OMV membrane remains stable. This suggests that such vesicles can be used as containers for the delivery of cationic drug molecules.

ACKNOWLEDGMENTS

This research was funded by the Russian Science Foundation, Grant No. 23-74-01005 (https://rscf.ru/en/project/23-74-01005/).

REFERENCES

1. Tang K.W.K., Millar B.C., Moore J.E. Antimicrobial Resistance (AMR). *Br. J. Biomed. Sci.* 2023. V. 80. P. 11387. doi: 10.3389/bjbs.2023.11387
2. Cox G., Wright G.D. Intrinsic Antibiotic Resistance: Mechanisms, Origins, Challenges and Solutions. *Int. J. Med. Microbiol.* 2013. V. 303. P. 287–292. doi: 10.1016/j.ijmm.2013.02.009
3. Lee C.-R., Lee J.H., Park M., Park K.S., Bae I.K., Kim Y.B., Cha C.-J., Jeong B.C., Lee S.H. Biology of Acinetobacter Baumannii: Pathogenesis, Antibiotic Resistance Mechanisms, and Prospective Treatment Options. *Front. Cell. Infect. Microbiol.* 2017. V. 7. P. 55. doi: 10.3389/fcimb.2017.00055
4. Olaitan A.O., Morand S., Rolain J.-M. Mechanisms of Polymyxin Resistance: Acquired and Intrinsic Resistance in Bacteria. *Front. Microbiol.* 2014. V. 5. P. 643. doi: 10.3389/fmicb.2014.00643

5. Langsrud S., Sundheim G., Borgmann-Strahsen R. Intrinsic and Acquired Resistance to Quaternary Ammonium Compounds in Food-Related Pseudomonas Spp. *J. Appl. Microbiol.* 2003. V. 95. P. 874–882. doi: 10.1046/j.1365-2672.2003.02064.x
6. Nikaido H. Molecular Basis of Bacterial Outer Membrane Permeability Revisited. *Microbiol. Mol. Biol. Rev.* 2003. V. 67. P. 593–656. doi: 10.1128/MMBR.67.4.593-656.2003
7. Khalid S., Schroeder C., Bond P.J., Duncan A.L. What Have Molecular Simulations Contributed to Understanding of Gram-Negative Bacterial Cell Envelopes? *Microbiology.* 2022. V. 168. doi: 10.1099/mic.0.001165
8. Kulp A., Kuehn M.J. Biological Functions and Biogenesis of Secreted Bacterial Outer Membrane Vesicles. *Annu. Rev. Microbiol.* 2010. V. 64. P. 163–184. doi: 10.1146/annurev.micro.091208.073413
9. Kuehn M.J., Kesty N.C. Bacterial Outer Membrane Vesicles and the Host–Pathogen Interaction. *Genes Dev.* 2005. V. 19. P. 2645–2655. doi: 10.1101/gad.1299905
10. Schwechheimer C., Kuehn M.J. Outer-Membrane Vesicles from Gram-Negative Bacteria: Biogenesis and Functions. *Nat. Rev. Microbiol.* 2015. V. 13. P. 605–619. doi: 10.1038/nrmicro3525
11. Li N.; Wu M.; Wang L.; Tang M.; Xin H.; Deng K. Efficient Isolation of Outer Membrane Vesicles (OMVs) Secreted by Gram-Negative Bacteria via a Novel Gradient Filtration Method. *Membranes.* 2024. V. 14. P. 135. doi: 10.3390/membranes14060135
12. Anand D., Chaudhuri A. Bacterial Outer Membrane Vesicles: New Insights and Applications. *Mol. Membr. Biol.* 2016. V. 33. P. 125–137. doi: 10.1080/09687688.2017.1400602
13. Magaña G., Harvey C., Taggart C.C., Rodgers A.M. Bacterial Outer Membrane Vesicles: Role in Pathogenesis and Host-Cell Interactions. *Antibiotics.* 2023. V. 13. P. 32. doi: 10.3390/antibiotics13010032
14. Kim J.Y., Suh J.W., Kang J.S., Kim S.B., Yoon Y.K., Sohn J.W. Gram-Negative Bacteria's Outer Membrane Vesicles. *Infect. Chemother.* 2023. V. 55. P. 1. doi: 10.3947/ic.2022.0145
15. Jan A.T. Outer Membrane Vesicles (OMVs) of Gram-Negative Bacteria: A Perspective Update. *Front. Microbiol.* 2017. V. 8. P. 1053. doi: 10.3389/fmicb.2017.01053
16. Muñoz-Echeverri L.M., Benavides-López S., Geiger O., Trujillo-Roldán M.A., Valdez-Cruz N.A. Bacterial Extracellular Vesicles: Biotechnological Perspective for Enhanced Productivity. *World J. Microbiol. Biotechnol.* 2024. V. 40. P. 174. doi: 10.1007/s11274-024-03963-7
17. Combo S., Mendes S., Nielsen K.M., Da Silva G.J., Domingues S. The Discovery of the Role of Outer Membrane Vesicles against Bacteria. *Biomedicines.* 2022. V. 10. P. 2399. doi: 10.3390/biomedicines10102399
18. Wai S.N., Takade A., Amako K. The Release of Outer Membrane Vesicles from the Strains of Enterotoxigenic *Escherichia coli*. *Microbiol. Immunol.* 1995. V. 39. P. 451–456. doi: 10.1111/j.1348-0421.1995.tb02228.x
19. Kolling G.L.; Matthews K.R. Export of Virulence Genes and Shiga Toxin by Membrane Vesicles of *Escherichia coli* O157:H7. *Appl. Environ. Microbiol.* 1999. V. 65. P. 1843–1848. doi: 10.1128/AEM.65.5.1843-1848.1999
20. Chatterjee D., Chaudhuri K. Association of Cholera Toxin with *Vibrio Cholerae* Outer Membrane Vesicles Which Are Internalized by Human Intestinal Epithelial Cells. *FEBS Lett.* 2011. V. 585. P. 1357–1362. doi: 10.1016/j.febslet.2011.04.017
21. Pérez A., Merino M., Rumbo-Feal S., Álvarez-Fraga L., Vallejo J.A., Beceiro A., Ohneck E.J., Mateos J., Fernández-Puente P., Actis L.A. et al. The FhaB/FhaC Two-Partner Secretion System Is Involved in Adhesion of *Acinetobacter Baumannii* AbH12O-A2 Strain. *Virulence.* 2017. V. 8. P. 959–974. doi: 10.1080/21505594.2016.1262313

22. Bauman S.J., Kuehn M.J. *Pseudomonas aeruginosa* Vesicles Associate with and Are Internalized by Human Lung Epithelial Cells. *BMC Microbiol.* 2009. V. 9. P. 26. doi: 10.1186/1471-2180-9-26
23. Ellis T.N., Kuehn M.J. Virulence and Immunomodulatory Roles of Bacterial Outer Membrane Vesicles. *Microbiol. Mol. Biol. Rev.* 2010. V. 74. P. 81–94. doi: 10.1128/MMBR.00031-09
24. Toledo A., Coleman J.L., Kuhlow C.J., Crowley J.T., Benach J.L. The Enolase of Borrelia Burgdorferi Is a Plasminogen Receptor Released in Outer Membrane Vesicles. *Infect. Immun.* 2012. V. 80. P. 359–368. doi: 10.1128/IAI.05836-11
25. Lappann M., Otto A., Becher D., Vogel U. Comparative Proteome Analysis of Spontaneous Outer Membrane Vesicles and Purified Outer Membranes of *Neisseria meningitidis*. *J. Bacteriol.* 2013. V. 195. P. 4425–4435. doi: 10.1128/JB.00625-13
26. Nagakubo T., Nomura N., Toyofuku M. Cracking Open Bacterial Membrane Vesicles. *Front. Microbiol.* 2020. V. 10. P. 3026. doi: 10.3389/fmicb.2019.03026
27. Yonezawa H., Osaki T., Kurata S., Fukuda M., Kawakami H., Ochiai K., Hanawa T., Kamiya S. Outer Membrane Vesicles of *Helicobacter pylori* TK1402 Are Involved in Biofilm Formation. *BMC Microbiol.* 2009. V. 9. P. 197. doi: 10.1186/1471-2180-9-197
28. Henriquez T., Falciani C. Extracellular Vesicles of Pseudomonas: Friends and Foes. *Antibiotics*. 2023. V. 12. P. 703. doi: 10.3390/antibiotics12040703
29. Jiang B., Lai Y., Xiao W., Zhong T., Liu F., Gong J., Huang J. Microbial Extracellular Vesicles Contribute to Antimicrobial Resistance. *PLOS Pathog.* 2024. V. 20. P. e1012143. doi: 10.1371/journal.ppat.1012143
30. Medvedeva E.S., Baranova N.B., Mouzykantov A.A., Grigorieva T.Yu., Davydova M.N., Trushin M.V., Chernova O.A., Chernov V.M. Adaptation of Mycoplasmas to Antimicrobial Agents: *Acholeplasma laidlawii* Extracellular Vesicles Mediate the Export of Ciprofloxacin and a Mutant Gene Related to the Antibiotic Target. *Sci. World J.* 2014. V. 2014. P. 1–7. doi: 10.1155/2014/150615
31. Kadurugamuwa J.L., Beveridge T.J. Bacteriolytic Effect of Membrane Vesicles from *Pseudomonas aeruginosa* on Other Bacteria Including Pathogens: Conceptually New Antibiotics. *J. Bacteriol.* 1996. V. 178. P. 2767–2774. doi: 10.1128/jb.178.10.2767-2774.1996
32. Manning A.J., Kuehn M.J. Contribution of Bacterial Outer Membrane Vesicles to Innate Bacterial Defense. *BMC Microbiol.* 2011. V. 11. P. 258. doi: 10.1186/1471-2180-11-258
33. Balhuizen M.D., Van Dijk A., Jansen J.W.A., Van De Lest C.H.A., Veldhuizen E.J.A., Haagsman H.P. Outer Membrane Vesicles Protect Gram-Negative Bacteria against Host Defense Peptides. *mSphere*. 2021. V. 6. P. e00523-21. doi: 10.1128/mSphere.00523-21
34. Park J., Kim M., Shin B., Kang M., Yang J., Lee T.K., Park W. A Novel Decoy Strategy for Polymyxin Resistance in *Acinetobacter baumannii*. *eLife*. 2021. V. 10. P. e66988. doi: 10.7554/eLife.66988
35. Grenier D., Bertrand J., Mayrand D. *Porphyromonas gingivalis* Outer Membrane Vesicles Promote Bacterial Resistance to Chlorhexidine. *Oral Microbiol. Immunol.* 1995. V. 10. P. 319–320. doi: 10.1111/j.1399-302X.1995.tb00161.x
36. Kim S.W., Park S.B., Im S.P., Lee J.S., Jung J.W., Gong T.W., Lazarte J.M.S., Kim J., Seo J.-S., Kim J.-H. et al. Outer Membrane Vesicles from β-Lactam-Resistant *Escherichia coli* Enable the Survival of β-Lactam-Susceptible *E. coli* in the Presence of β-Lactam Antibiotics. *Sci. Rep.* 2018. V. 8. P. 5402. doi: 10.1038/s41598-018-23656-0
37. Stentz R., Horn N., Cross K., Salt L., Brearley C., Livermore D.M., Carding S.R. Cephalosporinases Associated with Outer Membrane Vesicles Released by Bacteroides Spp. Protect Gut Pathogens and Commensals against β-Lactam Antibiotics. *J. Antimicrob. Chemother.* 2015. V. 70. P. 701–709. doi: 10.1093/jac/dku466

38. Marrink S.J., Risselada H.J., Yefimov S., Tieleman D.P., De Vries A.H. The MARTINI Force Field: Coarse Grained Model for Biomolecular Simulations. *J. Phys. Chem. B.* 2007. V. 111. P. 7812–7824. doi: 10.1021/jp071097f
39. Hsu P., Bruininks B.M.H., Jefferies D., Cesar Telles De Souza P., Lee J., Patel D.S., Marrink S.J., Qi Y., Khalid S., Im W. CHARMM-GUI Martini Maker for Modeling and Simulation of Complex Bacterial Membranes with Lipopolysaccharides. *J. Comput. Chem.* 2017. V. 38. P. 2354–2363. doi: 10.1002/jcc.24895
40. Jefferies D., Shearer J., Khalid S. Role of O-Antigen in Response to Mechanical Stress of the *E. coli* Outer Membrane: Insights from Coarse-Grained MD Simulations. *J. Phys. Chem. B.* 2019. V. 123. P. 3567–3575. doi: 10.1021/acs.jpcb.8b12168
41. Im W., Khalid S. Molecular Simulations of Gram-Negative Bacterial Membranes Come of Age. *Annu. Rev. Phys. Chem.* 2020. V. 71. P. 171–188. doi: 10.1146/annurev-physchem-103019-033434
42. Rzepiela A.J., Sengupta D., Goga N., Marrink S.J. Membrane Poration by Antimicrobial Peptides Combining Atomistic and Coarse-Grained Descriptions. *Faraday Discuss.* 2010. V. 144. P. 431–443. doi: 10.1039/B901615E
43. Balatti G., Ambroggio E., Fidelio G., Martini M., Pickholz M. Differential Interaction of Antimicrobial Peptides with Lipid Structures Studied by Coarse-Grained Molecular Dynamics Simulations. *Molecules.* 2017. V. 22. P. 1775. doi: 10.3390/molecules22101775
44. Talandashti R., Mehrnejad F., Rostamipour K., Doustdar F., Lavasanifar A. Molecular Insights into Pore Formation Mechanism, Membrane Perturbation, and Water Permeation by the Antimicrobial Peptide Pleurocidin: A Combined All-Atom and Coarse-Grained Molecular Dynamics Simulation Study. *J. Phys. Chem. B.* 2021. V. 125. P. 7163–7176. doi: 10.1021/acs.jpcb.1c01954
45. Lee H. Heterodimer and Pore Formation of Magainin 2 and PGLa: The Anchoring and Tilting of Peptides in Lipid Bilayers. *Biochim. Biophys. Acta BBA – Biomembr.* 2020. V. 1862. P. 183305. doi: 10.1016/j.bbamem.2020.183305.
46. Balatti G.E., Martini M.F., Pickholz M. A Coarse-Grained Approach to Studying the Interactions of the Antimicrobial Peptides Aurein 1.2 and Maculatin 1.1 with POPG/POPE Lipid Mixtures. *J. Mol. Model.* 2018. V. 24. P. 208. doi: 10.1007/s00894-018-3747-z
47. Catte A., Wilson M.R., Walker M., Oganesyan V.S. Antimicrobial Action of the Cationic Peptide, Chrysophsin-3: A Coarse-Grained Molecular Dynamics Study. *Soft Matter.* 2018. V. 14. P. 2796–2807. doi: 10.1039/C7SM02152F
48. Li Q., Zhong X., Sun L., Dai L. Enhancement of Cell Membrane Poration by the Antimicrobial Peptide Melp5. *arXiv:2310.11156 [physics.bio-ph]*. 2024. doi: 10.48550/arXiv.2310.11156
49. Melcrová A., Maity S., Melcr J., De Kok N.A.W., Gabler M., Van Der Eyden J., Stensen W., Svendsen J.S.M., Driessen A.J.M., Marrink S.J. et al. Lateral Membrane Organization as Target of an Antimicrobial Peptidomimetic Compound. *Nat. Commun.* 2023. V. 14. P. 4038. doi: 10.1038/s41467-023-39726-5
50. Hsu P.-C., Jefferies D., Khalid S. Molecular Dynamics Simulations Predict the Pathways via Which Pristine Fullerenes Penetrate Bacterial Membranes. *J. Phys. Chem. B.* 2016. V. 120. P. 11170–11179. doi: 10.1021/acs.jpcb.6b06615
51. Rietschel E.T., Kirikae T., Schade F.U., Mamat U., Schmidt G., Loppnow H., Ulmer A.J., Zähringer U., Seydel U., Di Padova F. et al. Bacterial Endotoxin: Molecular Relationships of Structure to Activity and Function. *FASEB J.* 1994. V. 8. P. 217–225. doi: 10.1096/fasebj.8.2.8119492
52. Van Oosten B., Marquardt D., Harroun T.A. Testing High Concentrations of Membrane Active Antibiotic Chlorhexidine Via Computational Titration and Calorimetry. *J. Phys. Chem. B.* 2017. V. 121. P. 4657–4668. doi: 10.1021/acs.jpcb.6b12510

53. Yesylevskyy S.O., Schäfer L.V., Sengupta D., Marrink S.J. Polarizable Water Model for the Coarse-Grained MARTINI Force Field. *PLoS Comput. Biol.* 2010. V. 6. P. e1000810. doi: 10.1371/journal.pcbi.1000810
54. Abraham M.J., Murtola T., Schulz R., Páll S., Smith J.C., Hess B., Lindahl E. GROMACS: High Performance Molecular Simulations through Multi-Level Parallelism from Laptops to Supercomputers. *SoftwareX*. 2015. V. 1. No. 2. P. 19–25. doi: 10.1016/j.softx.2015.06.001
55. Kovalenko I.B., Knyazeva O.S., Antal T.K., Ponomarev V.Y., Riznichenko G.Y., Rubin A.B. Multiparticle Brownian Dynamics Simulation of Experimental Kinetics of Cytochrome *Bf* Oxidation and Photosystem I Reduction by Plastocyanin. *Physiol. Plant.* 2017. V. 161. P. 88–96. doi: 10.1111/ppl.12570
56. Fedorov V.A., Kovalenko I.B., Khruschev S.S., Ustinin D.M., Antal T.K., Riznichenko G.Y., Rubin A.B. Comparative Analysis of Plastocyanin–Cytochrome *f* Complex Formation in Higher Plants, Green Algae and Cyanobacteria. *Physiol. Plant.* 2019. V. 166. P. 320–335. doi: 10.1111/ppl.12940
57. *The PyMOL Molecular Graphics System*, Version 2.4 Schrödinger, LLC.
58. Orekhov P.S., Kholina E.G., Bozdaganyan M.E., Nesterenko A.M., Kovalenko I.B., Strakhovskaya M.G. Molecular Mechanism of Uptake of Cationic Photoantimicrobial Phthalocyanine across Bacterial Membranes Revealed by Molecular Dynamics Simulations. *J. Phys. Chem. B.* 2018. V. 122. P. 3711–3722. doi: 10.1021/acs.jpcb.7b11707
59. Kholina E.G., Kovalenko I.B., Bozdaganyan M.E., Strakhovskaya M.G., Orekhov P.S. Cationic Antiseptics Facilitate Pore Formation in Model Bacterial Membranes. *J. Phys. Chem. B.* 2020. V. 124. P. 8593–8600. doi: 10.1021/acs.jpcb.0c07212
60. Meerovich G.A., Akhlyustina E.V., Romanishkin I.D., Makarova E.A., Tiganova I.G., Zhukhovitsky V.G., Kholina E.G., Kovalenko I.B., Romanova Y.M., Loschenov V.B. et al. Photodynamic Inactivation of Bacteria: Why It Is Not Enough to Excite a Photosensitizer. *Photodiagnosis Photodyn. Ther.* 2023. V. 44. P. 103853. doi: 10.1016/j.pdpdt.2023.103853
61. Zgurskaya H.I., Rybenkov V.V. Permeability Barriers of Gram-negative Pathogens. *Ann. N. Y. Acad. Sci.* 2020. V. 1459. P. 5–18. doi: 10.1111/nyas.14134
62. Maher C., Hassan K.A. The Gram-Negative Permeability Barrier: Tipping the Balance of the in and the Out. *mBio.* 2023. V. 14. P. e01205-23. doi: 10.1128/mbio.01205-23
63. González-Fernández C., Bringas E., Oostenbrink C., Ortiz I. *In silico* Investigation and Surmounting of Lipopolysaccharide Barrier in Gram-Negative Bacteria: How Far Has Molecular Dynamics Come? *Comput. Struct. Biotechnol. J.* 2022. V. 20. P. 5886–5901. doi: 10.1016/j.csbj.2022.10.039
64. Pier G. *Pseudomonas aeruginosa* Lipopolysaccharide: A Major Virulence Factor, Initiator of Inflammation and Target for Effective Immunity. *Int. J. Med. Microbiol.* 2007. V. 297. P. 277–295. doi: 10.1016/j.ijmm.2007.03.012
65. Makin S.A., Beveridge T.J. *Pseudomonas aeruginosa* PAO1 Ceases to Express Serotype-Specific Lipopolysaccharide at 45 Degrees C. *J. Bacteriol.* 1996. V. 178. P. 3350–3352. doi: 10.1128/jb.178.11.3350-3352.1996
66. King J.D., Kocíncová D., Westman E.L., Lam J.S. Review: Lipopolysaccharide Biosynthesis in *Pseudomonas aeruginosa*. *Innate Immun.* 2009. V. 15. P. 261–312. doi: 10.1177/1753425909106436
67. Vereshchagin A.N., Frolov N.A., Egorova K.S., Seitkalieva M.M., Ananikov V.P. Quaternary Ammonium Compounds (QACs) and Ionic Liquids (ILs) as Biocides: From Simple Antiseptics to Tunable Antimicrobials. *Int. J. Mol. Sci.* 2021. V. 22. P. 6793. doi: 10.3390/ijms22136793

68. Vejzovic D., Iftic A., Ön A., Semeraro E.F., Malanovic N. Octenidine's Efficacy: A Matter of Interpretation or the Influence of Experimental Setups? *Antibiotics.* 2022. V. 11. P. 1665. doi: 10.3390/antibiotics11111665
69. Nasrollahian S., Graham J.P., Halaji M. A Review of the Mechanisms That Confer Antibiotic Resistance in Pathotypes of *E. coli*. *Front. Cell. Infect. Microbiol.* 2024. V. 14. P. 1387497. doi: 10.3389/fcimb.2024.1387497

Received 17.07.2024.
Revised 27.07.2024.
Published 29.07.2024.

Катионные биоциды обладают тенденцией к встраиванию во внутренний монослой модельных везикул внешней мембраны грамотрицательных бактерий: результаты вычислительных экспериментов

Холина Е.Г., Коваленко И.Б., Страховская М.Г.

Московский государственный университет имени М.В. Ломоносова, Москва, Россия

Аннотация. Везикулы наружной мембраны (OMV), продуцируемые многими патогенными бактериями, играют важную роль в патогенезе бактерий. Они способствуют устойчивости бактерий к антибиотикам и действуют как естественные защитные барьеры. Изучение OMV важно как для понимания общих механизмов патогенности бактерий, так и для разработки антибактериальных препаратов. В этой статье мы создали молекулярно-динамическую модель везикулы, которая имитирует OMV грамотрицательных бактерий. Для исследования взаимодействия катионных антимикробных соединений с внешним липополисахаридным и внутренним фосфолипидным монослоями OMV, мы провели расчеты молекулярной динамики, помещая молекулы катионного антисептика октенидина снаружи или внутри модельной везикулы. Взаимодействие октенидина с внешним и внутренним монослоем существенно различалось: октенидин слабо взаимодействовал с внешней липополисахаридной поверхностью модельной OMV, но проявлял высокое сродство к фосфолипидам внутреннего монослоя. Чтобы изучить транслокацию катионных антимикробных молекул внутрь модельной OMV, мы провели серию расчетов неравновесной молекулярной динамики. Для всех трех катионных молекул биоцидов — антисептика октенидина, фотосенсибилизатора октакис(холинил)фталоцианина цинка и красителя метиленового синего — оказалось, что липополисахариды наружной мембраны OMV представляют барьер на пути проникновения биоцидов внутрь OMV, при этом конечным барьером являются фосфаты в составе молекул липида А.

Ключевые слова: *октенидин, октакис(холинил)фталоцианин цинка, метиленовый синий, грамотрицательные бактерии, везикулы наружной мембраны, липополисахариды, крупнозернистое моделирование, MARTINI.*